



Terrestrial Water Loss at Night: Global Relevance from Observations and Climate Models

Ryan S. Padrón¹, Lukas Gudmundsson¹, Dominik Michel¹, and Sonia I. Seneviratne¹

¹Institute for Atmospheric and Climate Science, Department of Environmental Systems Science, ETH Zurich, Zurich, 8092, Switzerland

Correspondence: Ryan S. Padrón (ryan.padron@env.ethz.ch)

Abstract. Nocturnal water loss (NWL) from the surface into the atmosphere is often overlooked because of the absence of solar radiation to drive evapotranspiration and the measuring difficulties involved. However, there is growing evidence that suggests NWL – and particularly nocturnal transpiration – represents a considerable fraction of the daily values. Here we provide a global overview of the characteristics of NWL based on latent heat flux estimates from the FLUXNET2015 dataset, 5 as well as from simulations of global climate models. Eddy-covariance measurements at 99 sites indicate that on average NWL represents 6.3 % of total evapotranspiration. There are six sites where NWL is higher than 15 %; these are mountain forests with considerable NWL during winter related to snowy and windy conditions. Higher vapor pressure deficit, wind speed and soil moisture are related to higher NWL, although this is not consistent across all sites. On the other hand, the global multi-model mean of terrestrial NWL is 7.9 % of total evapotranspiration. The spread of the model ensemble, however, is greater than 10 20 % over 70 % of the land area. Finally, the multi-model mean of future projections indicates an increase of NWL everywhere by an average of 1.8 %, but the spread between models at individual locations is often twice as large at least. Overall, this study highlights the relevance of water loss during the night and opens the door to explore its influence on the water cycle and the climate system under present and future conditions.

1 Introduction

15 Water is lost from the surface to the atmosphere through evapotranspiration (ET). This process interlinks the water, energy and carbon cycles, and hence influences climate, ecology, agriculture, and economy (e.g., Betts et al., 1996; Fisher et al., 2017; Zhang et al., 2015). Daytime ET, driven by solar radiation, represents the majority of the contribution to total water loss. On the other hand, it is recognized that vapor pressure deficit, temperature, wind speed and surface resistance also affect ET (Monteith, 1965; Penman, 1948). Moreover, it is night during half of each day on average. In consequence, nocturnal water loss can be 20 considerable and play a significant role for the surface water and energy balance.

In recent years there has been a growing body of evidence about the occurrence of nocturnal ET, with a specific focus on transpiration. Observations of nocturnal stomatal conductance have challenged the assumption of stomatal closure in the absence of photosynthetically active radiation (e.g., Daley and Phillips, 2006; Dawson et al., 2007; Snyder et al., 2003) – Lombardozzi et al. (2017) compiled evidence of this from 204 species. A review by Caird et al. (2007) estimated nocturnal



transpiration to be typically 5 % to 15 % of daytime rates, but sometimes as high as 30 %, based on studies using gas exchange measurements of individual leaves, whole-plant sap flow, and field scale lysimetry. More recently, Zeppel et al. (2014) refer to the ubiquity of nocturnal water fluxes and estimate nighttime transpiration to be 10–25 % of total daily transpiration. The above-mentioned publications stem from the plant physiology community, and the relevance of their results for hydrological
5 and climate studies is yet to be fully explored.

Total ET is of higher interest than transpiration from a water balance perspective. The best-established estimates of ET are from ground observations with lysimeters or eddy-covariance (EC) flux systems (e.g., Hirschi et al., 2017). Moreover, other estimates, for example from remote sensing, are not yet able to provide sufficient temporal resolution to study nocturnal water loss. Recently, Groh et al. (2019) reported annual nocturnal ET to be 3.5–9.5 % of annual daytime ET from lysimeter
10 measurements at two grass sites in Germany. Also using lysimeters, but under controlled environmental conditions, de Dios et al. (2015) quantified nocturnal water losses of 12–23 % of daytime values in row-crop monocultures of bean and cotton. On the other hand, EC estimates from one year in California showed 6 % of total ET during the night at an Oak-savanna site, and 1 % at a forested site (Fisher et al., 2007); whereas Novick et al. (2009) found nocturnal ET to be 8–9 % of mean daytime values at three co-located EC sites (two forests and one grassland) in the Southeastern United States.

15 Water is not only lost from the surface during the night, but it can also be gained by dew formation. For example, dew and hoar frost amounts to 4.2–6.4 % of annual precipitation in three humid grass sites in Austria and Germany (Groh et al., 2018, 2019), and was found to occur in approximately 30 % of the nights in a forest in central Colorado (Berkelhammer et al., 2013) and 70 % of the nights in a grassland in the Netherlands (Jacobs et al., 2006). Both ET and dew correspond to a latent heat flux and can prove difficult to disentangle depending on the temporal resolution of the data. In the present study, we therefore focus
20 on the net latent heat flux or net nocturnal water loss (NWL).

Models represent latent heat flux as a function of the air-surface gradient in specific humidity, aerodynamic resistance and surface resistance (corresponds to stomatal conductance over vegetated areas). Stomatal conductance is parameterized in most large-scale land surface models similarly to the Ball–Woodrow–Berry model (Ball et al., 1987; Ball, 1988; Collatz et al., 1991; Leuning, 1995; Medlyn et al., 2011; Sellers et al., 1996), i.e. as a linear function where the intercept represents
25 nocturnal conductance (see explanation in Lombardozzi et al., 2017). Underestimation of nocturnal stomatal conductance would lead to lower transpiration, and hence lower NWL. Previous research has noted that land surface models, dynamic global vegetation models and ecophysiological models continue to commonly assume that virtually no transpiration takes place at night, despite evidence suggesting otherwise (e.g., Lombardozzi et al., 2017; Zeppel et al., 2014). By adjusting the nocturnal stomatal conductance of the Community Land Model (CLM) version 4.5 based on empirical evidence, Lombardozzi
30 et al. (2017) obtain an increase of up to 5 % in global transpiration, as well as significant effects on soil moisture availability and carbon uptake. In another study, Vinukollu et al. (2011) reported a mean nocturnal ET from the VIC land surface model of 9.6 % relative to daytime ET. It is also known that common simple land evaporation models are not well suited for nocturnal conditions (Ershadi et al., 2014). Finally, to our knowledge, there have not been any studies analyzing NWL estimates from an ensemble of global climate models.



The goal of this study is to provide an overview of the magnitude and variability of NWL across the globe, as well as to explore its relationship to different meteorological and land cover conditions. An improved understanding of this overlooked flux is relevant for the surface water and energy balance. For this purpose, we analyze observations of NWL from a lysimeter and a global network of EC measurements, together with climate model estimates for present and projected future conditions.

5 2 Data

2.1 Observations

2.1.1 Co-located lysimeter and EC station

Water fluxes are measured by a co-located weighing lysimeter and EC tower (2 m height) at the Rietholzbach pre-alpine catchment in Northeastern Switzerland (47.38° N, 8.99° E; 795 m a.s.l.; see Seneviratne et al., 2012 for site details). The 10 sensors are thoroughly described by Hirschi et al. (2017). A threshold of 10 W m^{-2} for measured incoming solar radiation at the site is used to distinguish night from day. Data from 2010 to 2018 are used for comparing NWL estimates from these two independent measurement techniques.

For the lysimeter, changes in the total system mass (i.e. its weight plus accumulated seepage) are quantified every 5 minutes and correspond to water lost as ET or gained by precipitation, including dew. We apply an adaptive window and adaptive 15 threshold (AWAT) filter to the total system mass of the lysimeter to reduce noise in the timeseries (Peters et al., 2014; see also Ruth et al., 2018). A minimum of 5 minutes and maximum of 45 minutes are assumed for the moving-average window, as well as a minimum of 0.01 mm and a maximum of 0.25 mm for the threshold values to distinguish signal from noise. A piecewise cubic Hermitian spline is used to interpolate between points of significant mass change (Peters et al., 2016), after applying an 85th percentile “snap routine” at inflection points (Peters et al., 2017). We estimate dew from hourly weight increases in the 20 lysimeter when a co-located rain gauge does not record precipitation in that hour or the next. Nonetheless, if estimated dew surpasses a maximum formation rate of 0.07 mm h^{-1} (Monteith and Unsworth, 1990), it is instead attributed as rain or snow. NWL is calculated as ET minus dew. Lysimeter data from December to March are discarded because the quality is strongly 25 affected by formation of snow bridges and the occurrence of snow drift. In addition, data from the following months are also omitted due to cases with unrealistic lysimeter weight and/or seepage measurements: July–September 2017, August 2014 and 2016, and November 2010, 2011 and 2016.

The EC data are processed with EddyPro (LI-COR, 2018; Fratini and Mauder, 2014) to obtain a latent heat flux time series with a temporal resolution of 30 minutes. Values are discarded for intervals when rain occurs and for cases described by Hirschi et al. (2017), as well as for cases with too low turbulence (median threshold for friction velocity) based on Wutzler et al. (2018). The resulting gaps are filled according to Reichstein et al. (2005). Latent heat flux is converted into water volume by dividing 30 over the latent heat of vaporization; here we assume $\lambda = 2.472 \text{E}6 \text{ J kg}^{-1}$.



2.1.2 Global network of EC stations

To obtain a broader picture of NWL across the globe we employ the FLUXNET2015 Tier 1 dataset, which provides EC measurements of latent heat flux together with numerous other meteorological variables from a global network of 166 sites. We further select a subset of 99 stations that contain at least 3 years of data to obtain a more accurate climatology of NWL. The 5 temporal resolution of the data is 30 minutes. There are implemented tailored steps for quality assurance and quality control (Pastorello et al., 2014). A quality flag at each time interval indicates whether the data were measured or gap-filled based on marginal distribution sampling (Reichstein et al., 2005). Moreover, there is an energy balance closure correction factor applied to the data based on the assumption that the Bowen ratio is correct. Full details of the data processing are available at <https://fluxnet.fluxdata.org/data/fluxnet2015-dataset/data-processing/>. Even though the dataset distinguishes between daytime 10 and nighttime intervals based on potential incoming solar radiation, we additionally determine the total number of nighttime hours by calculating the sunset and sunrise time of each day (see <https://www.esrl.noaa.gov/gmd/grad/solcalc/calcdetails.html>).

It is important to be aware that the reliability of EC measurements decreases during the night due to low and intermittent turbulence (e.g., Baldocchi, 2003; Moffat et al., 2007). Nonetheless, on average across all analyzed sites, latent heat flux is measured in 60 % of all nighttime intervals, whereas gap-filling is required in the remaining 40 %. Furthermore, we acknowledge 15 the substantial and exhaustive work carried out to provide best estimates of the fluxes in the FLUXNET2015 dataset. Therefore, it is meaningful to employ this dataset to study NWL, but caution is required when interpreting the results.

2.2 Climate models

Sub-daily climate model output is required to study NWL. Here we analyze an ensemble of climate model simulations of the fifth phase of the Coupled Model Inter-comparison Project (CMIP5) that provide 3 hourly estimates of latent heat flux. As for 20 the EC data, we obtain NWL by dividing it over the latent heat of vaporization λ . For present conditions we use data from historical simulations during the period 1976–2005, whereas for the future period 2081–2100, we use data from simulations with the “business as usual” RCP8.5 emissions scenario (Moss et al., 2010). The employed ensemble comprises 26 different models (or model configurations) with one initial condition simulation (see Table A1). Data from all models are bilinearly interpolated to a common $2.5^\circ \times 2.5^\circ$ grid. Grid cells with data from less than 2/3 of all models are not considered.

25 To estimate total NWL we obtain the average flux from all 3 hourly intervals that are exclusively night, and then extrapolate this value based on the complete number of nocturnal hours. To achieve this, we compute the time of sunset and sunrise for each day at the center of each individual grid cell using the solar time equations without accounting for topography. Note that this extrapolation approach could lead to inaccuracies if the NWL rate from periods immediately following sunset or just prior to sunrise systematically differ from the NWL rate during the middle of the night.

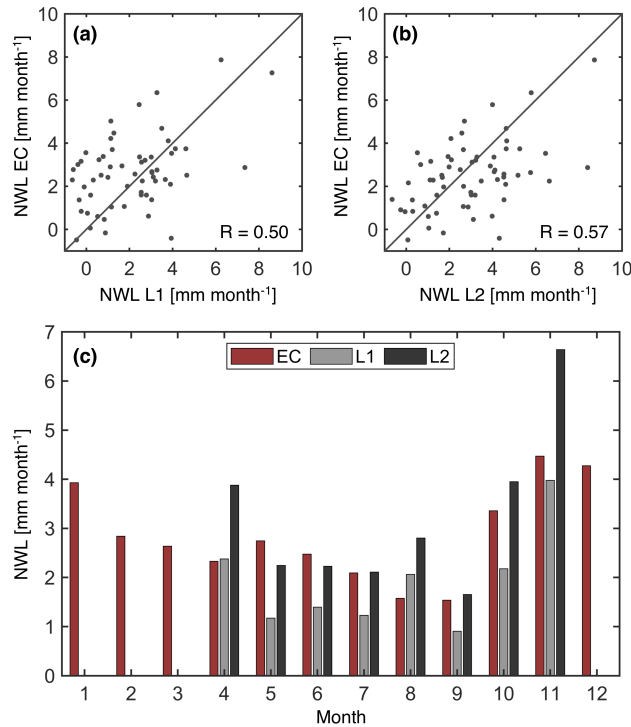


Figure 1. Comparison of nocturnal water loss (NWL) measured by the co-located lysimeter and EC system. Comparison of individual months is shown in (a) and (b) with the Pearson correlation coefficient denoted as R, whereas a comparison of the climatology from the period 2010–2018 is shown in (c). L1 corresponds to the lysimeter estimate with a maximum dew formation threshold of 0.07 mm h^{-1} , and L2 with a threshold of 0.035 mm h^{-1} . Lysimeter data from December to March are discarded because of measurements issues when snow is present.

3 Results

3.1 Observed nocturnal water loss

Monthly NWL from the co-located lysimeter and EC system show a Pearson correlation of 0.5–0.57 (Fig. 1), depending on how dew is estimated from the lysimeter data. As a sensitivity test, here we select a second threshold of 0.035 mm h^{-1} , in 5 addition to the defined value of 0.07 mm h^{-1} for maximum dew formation, when processing the lysimeter data. Note that the correlations may be affected by the difference in the footprint of the sensors and periods with gap-filled EC data. Also, in this case there is no energy balance closure correction factor applied to the EC data. The agreement between EC and lysimeter improves if the NWL monthly climatology is analyzed. Moreover, in months when one of the lysimeter estimates of NWL is either too high or too low relative to the EC data, the second lysimeter estimate generally has a much better agreement. Overall, 10 these results suggest that EC measurements can provide meaningful estimates of NWL. The annual climatology of EC-based NWL at this particular grassland site in Switzerland is 34.3 mm, equivalent to 5.8 % of annual ET.

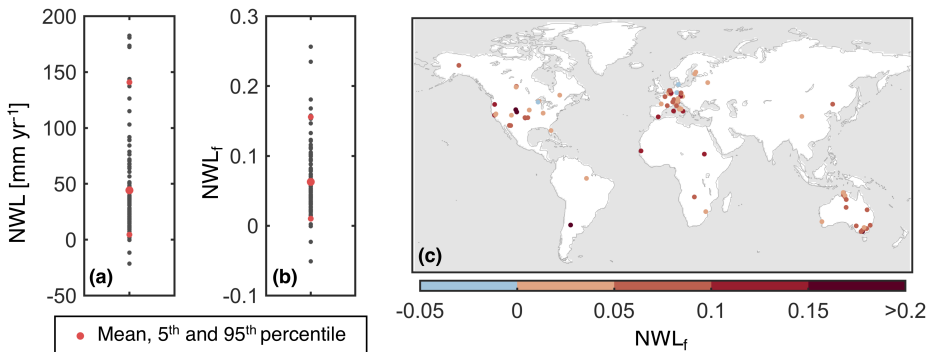


Figure 2. Nocturnal water loss at 99 FLUXNET sites: as the annual magnitude NWL (a), and as the fraction of total evapotranspiration NWL_f (b). (c) Spatial distribution of NWL_f.

An overview of observed NWL at the analyzed FLUXNET sites is presented in Fig. 2. Mean annual NWL is 44.2 mm on average over all 99 stations, whereas the 5th and 95th percentiles of the distribution are 4.5 mm and 140.9 mm. There is a positive Spearman correlation coefficient of 0.61 between total ET and NWL, indicating generally higher NWL at sites with higher ET. The net nocturnal water loss as a fraction of total ET, i.e. NWL_f = NWL / ET, provides more insight on the relevance 5 of the nocturnal water flux. Average NWL_f across all stations is 6.3 %, the 5th percentile is 1 %, and the 95th percentile is 15.6 %. These annual mean values are computed from monthly climatologies obtained by omitting months with half or more of missing latent heat flux data. Interannual variability of NWL_f, represented by the standard deviation, is 2.4 % on average from all sites. To analyze seasonality, we compute NWL for the trimesters December–February (DJF), March–May (MAM), 10 June–August (JJA) and September–November (SON) at all 81 sites located above 30° N, where seasonal differences are clearer, and data are available. The most common season with the highest NWL is winter (35.8 % of the sites) followed by autumn (25.9 %), summer (23.5 %) and spring (14.8 %); whereas for the lowest NWL, the most common is summer (37 %) and the least common is autumn (13.6 %). Note that this is partly related to an increase in the total nocturnal hours as we go from summer to autumn and winter.

The variability in NWL_f across sites is not easily explained by annual average climate conditions (temperature and precipitation) or land cover (Fig. 3). Nonetheless, deciduous broadleaf forests (DBF) have an overall lower NWL_f, whereas evergreen needleleaf forests (ENF) include most cases with higher NWL_f. An ANOVA test (differences in the mean) for the land cover categories has a p-value of 0.038, and a Kruskall-Wallis test (differences in the distribution) a p-value of 0.055. The three sites with negative NWL_f (dew is greater than nocturnal ET) are Hainich (Germany), Soroe (Denmark), and Willow Creek (WI, USA). These are all DBF with typically lower vapor pressure deficit and higher soil moisture than approximately 75 % of all 20 sites. On the other hand, there are six sites with NWL_f > 15 %: GLEES (WY, USA), GLEES Brooklyn tower (WY, USA), Niwot Ridge Forest (CO, USA), Lavarone (Italy), Wallaby Creek (Australia), and San Luis (Argentina). These are four ENF, an evergreen broadleaf forest (EBF) and a mixed forest (MF) in mountainous areas. Winter contribution to annual NWL approx-

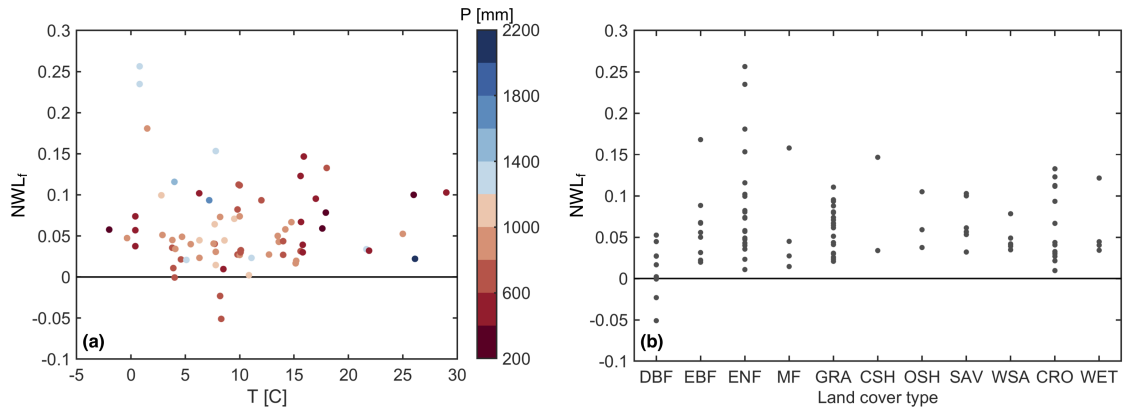


Figure 3. Relation of NWL_f with (a) mean annual temperature (T) and precipitation (P), and with (b) land cover type at FLUXNET sites. Precipitation and temperature data are available for 73 of the 99 FLUXNET sites. Land cover types are deciduous broadleaf forest (DBF), evergreen needleleaf forest (ENF), evergreen broadleaf forest (EBF), mixed forest (MF), grassland (GRA), closed shrubland (CSH), open shrubland (OSH), savanna (SAV), woody savanna (WSA), cropland (CRO), and wetland (WET).

imately doubles that of summer in the four ENF sites. Snowy and windy conditions at these sites may suggest a considerable contribution of sublimation to NWL.

At most sites there is a positive correlation of NWL with vapor pressure deficit (VPD), wind speed (WS) and soil moisture (SM) for the 30-minute data (Fig. 4). As expected, a higher evaporative demand (VPD), aerodynamical conductance (related to WS) and water supply (related to SM) generally favor higher NWL. Nonetheless, Spearman correlations at the majority of sites are lower than 0.3. Reasons for this may include confounding effects among the analyzed drivers of NWL, observational uncertainty and a possible physiological control (stomatal conductance) on nocturnal transpiration. Although there is no clear dependency of the correlations on land cover, we note that croplands often exhibit higher correlations with VPD and WS. When analyzing data from summer months, we find that four out of the nine sites showing the highest correlations with VPD are deciduous broadleaf forests, whereas the other five are irrigated crops. The irrigated crops also have the highest correlations with WS. Meanwhile the four sites with the highest correlations with SM are located in southern Arizona, a water limited region.

3.2 Climate model estimates of nocturnal water loss

The multi-model mean depicts an average NWL_f of 7.9 % across all land grid cells excluding desert regions and Greenland (Fig. 5). The 5th percentile of the spatial distribution without deserts and Greenland is 1.8 %, and the 95th percentile is 13.2 %. In tropical regions NWL_f is generally below the global average, even though NWL can e.g. surpass 80 mm yr⁻¹ in parts of the Amazon. Central and northern Europe, USA, China and India show similar regional averages of approximately 9 %. The models also suggest a high relevance of nocturnal water fluxes in Australia with an average NWL_f of 13.6 %, and in the Mediterranean with 12.5 %. In most of Greenland and parts of Egypt the amount of dew or hoar frost is greater than the water

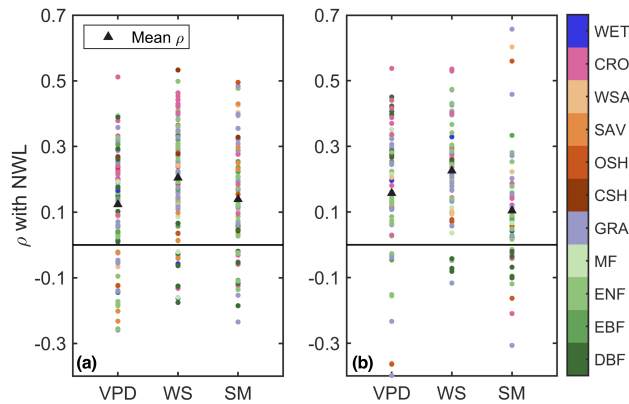


Figure 4. Spearman correlation (ρ) of 30-minute nocturnal water loss (NWL) with vapor pressure deficit (VPD), wind speed (WS) and soil moisture (SM) at FLUXNET sites. Panel (a) is for all data and (b) for summer months (JJA) at sites located above 30° N. Land cover types are deciduous broadleaf forest (DBF), evergreen needleleaf forest (ENF), evergreen broadleaf forest (EBF), mixed forest (MF), grassland (GRA), closed shrubland (CSH), open shrubland (OSH), savanna (SAV), woody savanna (WSA), cropland (CRO), and wetland (WET).

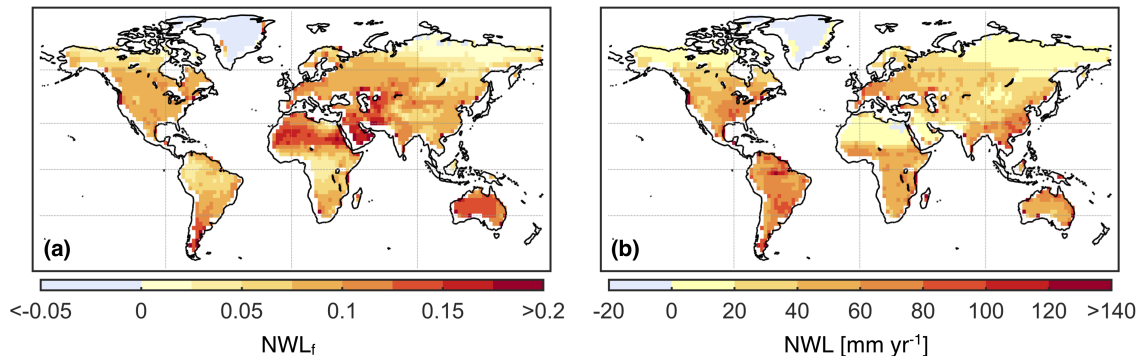


Figure 5. Map of multi-model mean NWL_f (a) and NWL (b).

lost through ET during the night. Interannual variability of NWL_f, given by the standard deviation of the 30-year time series from the multi-model mean, is below 2 % on 95 % of land grid cells excluding deserts and Greenland. Finally, we focus in the northern midlatitudes (30 – 60° N) to analyze seasonality. The multi-model mean indicates that autumn (SON) is the season with highest NWL on average (50.4 % of grid cells), whereas the lowest NWL typically corresponds to winter (DJF) (73 % of grid cells).

There are large discrepancies in NWL_f between the different climate models (Fig. 6). The 95th percentile of the model ensemble is higher than 15 % in most of the globe, whereas the 5th percentile even shows negative values (i.e. dew is greater than nocturnal ET) in parts of the tropics and high latitudes. The central 90 % spread of the ensemble is almost everywhere larger than 10 %, and even greater than 20 % in southern South America, eastern Africa, India and Australia. This means that

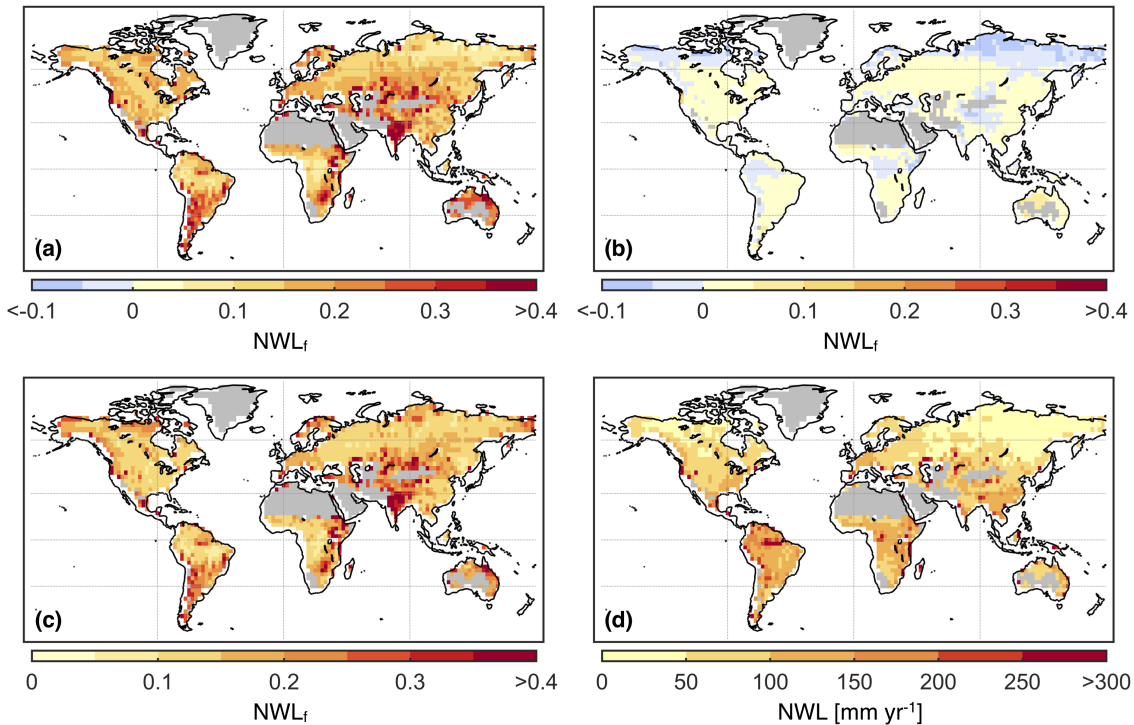


Figure 6. NWL_f uncertainty within the climate model ensemble. (a) Map of the 95th percentile of the ensemble. (b) Map of the 5th percentile of the ensemble. (c) Map of the central 90 % spread of the ensemble, i.e. the difference between (a) and (b). (d) Similar to (c) but for NWL instead of NWL_f.

at certain locations some models simulate NWL_f to be approximately zero, whereas estimates from other models are higher than 20 %. Even though the model differences in NWL_f can originate from differences in total ET (e.g. in India), we also find differences in NWL generally ranging from 50 to 150 mm yr⁻¹. The models inmcm4, EC-EARTH, NorESM1-M and CNRM-CM5 have systematically low values of NWL_f throughout the globe; whereas GISS-E2-R, GISS-E2-H and MIROC5 5 tend to simulate the highest values of NWL_f.

Terrestrial NWL_f is projected to increase towards the end of the century throughout the globe (Fig. 7). The average increase in the multi-model mean is 1.8 %, neglecting deserts and Greenland. Whereas NWL is projected to increase almost everywhere, this is not the case for total ET. In the Amazon, Central America, southern Africa and the Mediterranean, projected decreases in ET favor the increase in NWL_f. Another point to highlight is the effect of the nocturnal flux on future changes in ET. In 10 more than half of all land grid cells, the change in NWL is greater than 20 % of the absolute change in ET. Finally, we must note the high uncertainty associated with future changes in NWL_f. The spread of the ensemble is generally more than twice the magnitude of the increase projected by the multi-model mean, reducing confidence even in the sign of future changes.

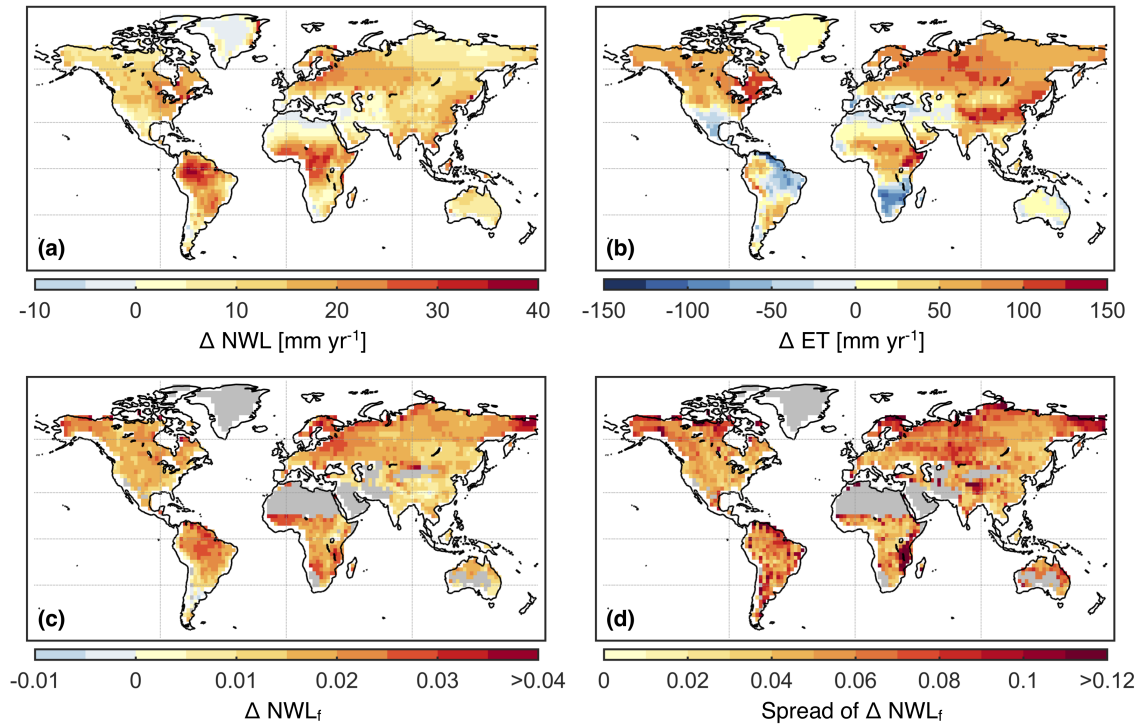


Figure 7. Multi-model mean of projected changes in NWL (a), total ET (b) and NWL_f (c) for the period 2081–2100 relative to the period 1976–2005. (d) Central 90 % spread of the ensemble for projected changes in NWL_f.

3.3 Comparison of observed and simulated nocturnal water loss

We compare the site-level EC observations to model estimates from the corresponding grid cells. Modelled NWL_f generally shows an overestimation, although there are a few exceptions (Fig. 8a) – the average from the considered grid cells is 10.6 %, whereas the observational average is 7 %. Interestingly, the multi-model mean has a smaller spread across sites than 5 observations. This is partly explained by strong local discrepancies between individual models causing little variability in the multi-model mean; nonetheless, it could also be related to smoothing of cross-site differences in the much coarser spatial resolution of the models. At locations above 30° N, where most stations are found and seasonal differences are clearer, the simulated seasonal behavior agrees generally well with that of the EC data (Fig. 8b, see also Fig. S1). However, there is a noteworthy overestimation of the cases where the multi-model mean shows the lowest NWL to occur in summer, which is 10 compensated by an underestimation for autumn and spring.

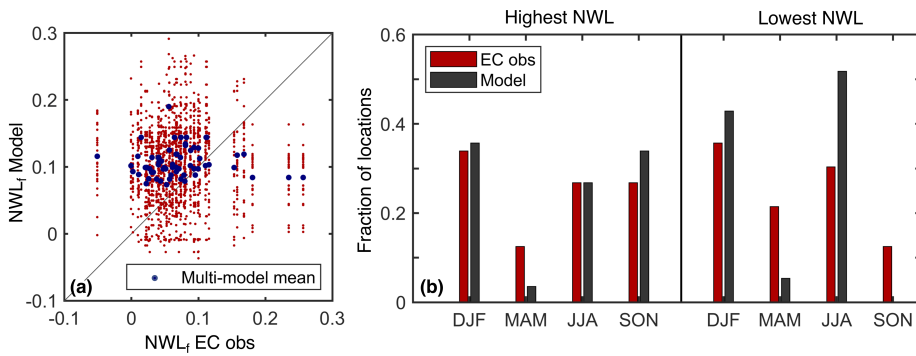


Figure 8. Comparison of observations with climate model simulations at the corresponding grid cells. (a) NWL_f from EC observations versus model simulations at 64 locations. (b) Fraction of locations (i.e. FLUXNET sites or grid cells) above 30°N where each season has the highest or lowest NWL on average. Seasons are defined by the trimesters December–February (DJF), March–May (MAM), June–August (JJA) and September–November (SON).

4 Discussion and conclusions

Our average estimate of net nocturnal water loss relative to total evapotranspiration from 99 FLUXNET sites is 6.3 %. This is smaller than reported values around 10–25 % from published physiological studies (Zeppel et al., 2014). However, it is important to distinguish that our focus is on the net flux, i.e. evapotranspiration minus dew, whereas physiological studies refer 5 only to transpiration. The results agree with the expectation of lower NWL_f when dew is taken into account. In addition, we recall that nocturnal measurements at FLUXNET stations can be affected by low-turbulence conditions, and therefore gap-filled and energy-balance-corrected data are used in the analysis. Future work could help to disentangle the distinct fluxes of transpiration, evaporation from soil and canopy, sublimation and dew during the night.

We find that higher vapor pressure deficit, wind speed and soil moisture tend to favor higher NWL , although the correlations 10 are rather low. Similar results were reported by Groh et al. (2019) at two sites in Germany. Dawson et al. (2007) also found these conditions to favor higher nocturnal sap flow in woody plant species from different ecosystems, but in their case the relationships are much clearer. Meanwhile, Zeppel et al. (2014) points to plant functional type, ecosystem type, and biotic temporal characteristics like leaf or stand age, as possible additional factors influencing NWL . On the other hand, de Dios et al. 15 (2015) found no temporal relation with vapor pressure deficit because of endogenous circadian regulation in an experiment with crops under controlled environmental conditions. Additionally, an increase in nocturnal sap flow and stomatal conductance was reported in two tree species under increased atmospheric CO_2 concentration, given sufficient soil moisture (Zeppel et al., 2011, 2012). Further research about the controls of NWL , and in particular nocturnal transpiration, is required.

The climate model ensemble provides an average NWL_f of 7.9 % over land, which is slightly higher than the observational 20 estimate. Moreover, the overestimation is greater when considering only grid cells that contain FLUXNET locations. These relatively high multi-model mean estimates of NWL_f are surprising given the literature that suggests models underestimate nocturnal stomatal conductance. Note that increasing model nocturnal stomatal conductance would likely lead to even higher



values of simulated NWL_f . Thus, it is possible that even if the mean simulated magnitude of nocturnal water loss is relatively accurate, the underlying processes may be misrepresented.

Our analysis indicates strong discrepancies between individual models in simulated NWL_f , which are much larger than the spatial and inter-annual variability. Note that differences in NWL can represent a substantial fraction of model differences in total ET. We also find that model differences in NWL are highly correlated to model differences in near surface air temperature during the night (Fig. S2). These biases could further affect boundary layer evolution and precipitation timing in models. Model uncertainty also reduces confidence in the direction of change in NWL under global warming, despite the multi-model mean showing a projected increase throughout the world.

In conclusion, our study provides a comprehensive global overview of NWL – defined as nocturnal evapotranspiration minus dew – from observations and climate models. The magnitude of this flux suggests it can be important for the surface energy and water balance, and therefore relevant to consider in hydroclimate analyses. Future research about NWL focused at seasonal and shorter timescales could address its influence on climate impacts during extreme conditions (e.g., Duarte et al., 2016; Groh et al., 2019). Finally, ongoing development and expansion in sensing water and energy fluxes are expected to help address the uncertainties we have highlighted around NWL through continued research on this topic.

15 *Data availability.* The FLUXNET2015 dataset is available at <https://fluxnet.fluxdata.org/data/fluxnet2015-dataset/>. The CMIP5 data used in this study are available at <https://esgf-node.llnl.gov/projects/esgf-llnl/>. Processed hourly data from the co-located lysimeter and EC tower at Rietholzbach, as well as accompanying meteorological data, are available through a link shared with the handling editor (upon final publication these data will be available at a suitable repository).



Appendix A: List of climate models used in the analysis

Table A1. Climate models or model configurations employed for the analysis. Note that there are slight variations depending on time period / scenario and on variable under consideration.

Model	Simulation	1976–2005: Historical		2081–2100: RCP8.5	
		Latent heat flux	Temperature	Latent heat flux	Temperature
ACCESS1-0	r1i1p1	X	X	X	
ACCESS1-3	r1i1p1	X	X	X	
bcc-csm1-1	r1i1p1	X	X	X	
bcc-csm1-1-m	r1i1p1	X	X	X	
BNU-ESM	r1i1p1	X	X	X	
CCSM4	r6i1p1	X	X	X	
CMCC-CM	r1i1p1	X	X	X	
CNRM-CM5	r1i1p1	X	X	X	
EC-EARTH	r2i1p1	X	X	X	
FGOALS-g2	r1i1p1	X	X	X	
FGOALS-s2	r1i1p1	X			
GFDL-CM3	r1i1p1	X	X	X	
GFDL-ESM2G	r1i1p1	X	X	X	
GFDL-ESM2M	r1i1p1	X	X		
GISS-E2-H	r6i1p1	X	X	X	
GISS-E2-R	r6i1p1	X	X	X	
HadGEM2-ES	r2i1p1	X	X		
inmcm4	r1i1p1	X	X	X	
IPSL-CM5A-LR	r1i1p1	X	X	X	
IPSL-CM5A-MR	r1i1p1	X	X	X	
MIROC-ESM	r1i1p1	X	X	X	
MIROC-ESM-CHEM	r1i1p1	X	X	X	
MIROC5	r1i1p1	X	X	X	
MRI-CGCM3	r1i1p1	X	X	X	
MRI-ESM1	r1i1p1	X	X		
NorESM1-M	r1i1p1	X	X	X	



Author contributions. RSP, LG and SIS conceived the idea and designed the study. SIS acquired the funding to carry out the study. DM collected and processed the co-located lysimeter and EC data from the Swiss site. RSP processed the FLUXNET2015 and CMIP5 data. RSP performed the analysis and wrote the manuscript with contributions from all other authors throughout the study. All authors discussed the results, read and reviewed the manuscript.

5 *Competing interests.* The authors declare that they have no conflict of interest.

Acknowledgements. We acknowledge partial support from the H2020 CRESCENDO project (grant agreement 641816), and from the European Research Council (ERC) DROUGHT-HEAT project funded by the European Community's Seventh Framework Programme (grant agreement FP7-IDEAS-ERC-617518). This work used eddy covariance data acquired and shared by the FLUXNET community, including these networks: AmeriFlux, AfriFlux, AsiaFlux, CarboAfrica, CarboEuropeIP, CarboItaly, CarboMont, ChinaFlux, Fluxnet-Canada, Green-10 Grass, ICOS, KoFlux, LBA, NECC, OzFlux-TERN, TCOS-Siberia, and USCCC. The ERA-Interim reanalysis data are provided by ECMWF and processed by LSCE. The FLUXNET eddy covariance data processing and harmonization was carried out by the European Fluxes Database Cluster, AmeriFlux Management Project, and Fluxdata project of FLUXNET, with the support of CDIAC and ICOS Ecosystem Thematic Center, and the OzFlux, ChinaFlux and AsiaFlux offices. We acknowledge the World Climate Research Program's Working Group on Coupled Modelling, which is responsible for the Coupled Model Intercomparison Project (CMIP), and we thank the climate modelling 15 groups for producing and making available their model output. For CMIP, the US Department of Energy's Program for Climate Model Diagnosis and Intercomparison provides coordinating support and led development of software infrastructure in partnership with the Global Organization for Earth System Science Portals. We thank Urs Beyerle for downloading the CMIP5 data.



References

Baldocchi, D. D.: Assessing the eddy covariance technique for evaluating carbon dioxide exchange rates of ecosystems: past, present and future, *Glob. Chang. Biol.*, 9, 479–492, <https://doi.org/10.1046/j.1365-2486.2003.00629.x>, 2003.

Ball, J. T.: An Analysis of Stomatal Conductance, Stanford University, 1988.

5 Ball, J. T., Woodrow, I. E., and Berry, J. A.: A Model Predicting Stomatal Conductance and its Contribution to the Control of Photosynthesis under Different Environmental Conditions, in: *Prog. Photosynth. Res.*, edited by Biggins, J., pp. 221–224, Springer Netherlands, https://doi.org/doi:10.1007/978-94-017-0519-6_48, 1987.

Berkelhammer, M., Hu, J., Bailey, A., Noone, D. C., Still, C. J., Barnard, H., Gochis, D., Hsiao, G. S., Rahn, T., and Turnipseed, A.: The nocturnal water cycle in an open-canopy forest, *J. Geophys. Res. Atmos.*, 118, 10,225–10,242, <https://doi.org/10.1002/jgrd.50701>, 2013.

10 Betts, A. K., Ball, J. H., Beljaars, A. C. M., Miller, M. J., and Viterbo, P. A.: The land surface-atmosphere interaction: A review based on observational and global modeling perspectives, *J. Geophys. Res. Atmos.*, 101, 7209–7225, <https://doi.org/10.1029/95JD02135>, 1996.

Caird, M. A., Richards, J. H., and Donovan, L. A.: Nighttime stomatal conductance and transpiration in C3 and C4 plants., *Plant Physiol.*, 143, 4–10, <https://doi.org/10.1104/pp.106.092940>, 2007.

15 Collatz, G. J., Ball, J. T., Grivet, C., and Berry, J. A.: Physiological and environmental regulation of stomatal conductance, photosynthesis and transpiration: a model that includes a laminar boundary layer, *Agric. For. Meteorol.*, 54, 107–136, [https://doi.org/doi:10.1016/0168-1923\(91\)90002-8](https://doi.org/doi:10.1016/0168-1923(91)90002-8), 1991.

Daley, M. J. and Phillips, N. G.: Interspecific variation in nighttime transpiration and stomatal conductance in a mixed New England deciduous forest, *Tree Physiol.*, 26, 411–419, <https://doi.org/10.1093/treephys/26.4.411>, 2006.

Dawson, T. E., Burgess, S. S. O., Tu, K. P., Oliveira, R. S., Santiago, L. S., Fisher, J. B., Simonin, K. A., and Ambrose, A. R.: Nighttime transpiration in woody plants from contrasting ecosystems, *Tree Physiol.*, 27, 561–575, <https://doi.org/10.1093/treephys/27.4.561>, 2007.

20 de Dios, V. R., Roy, J., Ferrio, J. P., Alday, J. G., Landais, D., Milcu, A., and Gessler, A.: Processes driving nocturnal transpiration and implications for estimating land evapotranspiration., *Sci. Rep.*, 5, 10975, <https://doi.org/10.1038/srep10975>, 2015.

Duarte, A. G., Katata, G., Hoshika, Y., Hossain, M., Kreuzwieser, J., Arneth, A., and Ruehr, N. K.: Immediate and potential long-term effects of consecutive heat waves on the photosynthetic performance and water balance in Douglas-fir, *J. Plant Physiol.*, 205, 57–66, <https://doi.org/10.1016/J.JPLPH.2016.08.012>, 2016.

25 Ershadi, A., McCabe, M., Evans, J., Chaney, N., and Wood, E.: Multi-site evaluation of terrestrial evaporation models using FLUXNET data, *Agric. For. Meteorol.*, 187, 46–61, <https://doi.org/10.1016/J.AGRFORMAT.2013.11.008>, 2014.

Fisher, J. B., Baldocchi, D. D., Misson, L., Dawson, T. E., and Goldstein, A. H.: What the towers don't see at night: nocturnal sap flow in trees and shrubs at two AmeriFlux sites in California, *Tree Physiol.*, 27, 597–610, 2007.

30 Fisher, J. B., Melton, F., Middleton, E., Hain, C., Anderson, M., Allen, R., McCabe, M. F., Hook, S., Baldocchi, D., Townsend, P. A., Kilic, A., Tu, K., Miralles, D. D., Perret, J., Lagouarde, J.-P., Waliser, D., Purdy, A. J., French, A., Schimel, D., Famiglietti, J. S., Stephens, G., and Wood, E. F.: The future of evapotranspiration: Global requirements for ecosystem functioning, carbon and climate feedbacks, agricultural management, and water resources, *Water Resour. Res.*, 53, 2618–2626, <https://doi.org/10.1002/2016WR020175>, 2017.

Fratini, G. and Mauder, M.: Towards a consistent eddy-covariance processing: an intercomparison of EddyPro and TK3, *Atmos. Meas. Tech.*, 7, 2273–2281, <https://doi.org/10.5194/amt-7-2273-2014>, 2014.

35 Groh, J., Slawitsch, V., Herndl, M., Graf, A., Vereecken, H., and Pütz, T.: Determining dew and hoar frost formation for a low mountain range and alpine grassland site by weighable lysimeter, *J. Hydrol.*, 563, 372–381, <https://doi.org/10.1016/J.JHYDROL.2018.06.009>, 2018.



Groh, J., Pütz, T., Gerke, H. H., Vanderborght, J., and Vereecken, H.: Quantification and Prediction of Nighttime Evapotranspiration for Two Distinct Grassland Ecosystems, *Water Resour. Res.*, 55, 2018WR024072, <https://doi.org/10.1029/2018WR024072>, 2019.

Hirschi, M., Michel, D., Lehner, I., and Seneviratne, S. I.: A site-level comparison of lysimeter and eddy covariance flux measurements of evapotranspiration, *Hydrol. Earth Syst. Sci.*, 21, 1809–1825, <https://doi.org/10.5194/hess-21-1809-2017>, 2017.

5 Jacobs, A. F., Heusinkveld, B. G., Kruit, R. J., and Berkowicz, S. M.: Contribution of dew to the water budget of a grassland area in the Netherlands, *Water Resour. Res.*, 42, <https://doi.org/10.1029/2005WR004055>, 2006.

Leuning, R.: A critical appraisal of a combined stomatal-photosynthesis model for C3 plants, *Plant, Cell Environ.*, 18, 339–355, <https://doi.org/10.1111/j.1365-3040.1995.tb00370.x>, 1995.

LI-COR, B.: Eddy Covariance Processing Software, www.licor.com/EddyPro, 2018.

10 Lombardozzi, D. L., Zeppel, M. J. B., Fisher, R. A., and Tawfik, A.: Representing nighttime and minimum conductance in CLM4.5: global hydrology and carbon sensitivity analysis using observational constraints, *Geosci. Model Dev.*, 10, 321–331, <https://doi.org/10.5194/gmd-10-321-2017>, 2017.

Medlyn, B. E., Duursma, R. A., Eamus, D., Ellsworth, D. S., Prentice, I. C., Barton, C. V. M., Crous, K. Y., De Angelis, P., Freeman, M., and Wingate, L.: Reconciling the optimal and empirical approaches to modelling stomatal conductance, *Glob. Chang. Biol.*, 17, 2134–2144, <https://doi.org/10.1111/j.1365-2486.2010.02375.x>, 2011.

15 Moffat, A. M., Papale, D., Reichstein, M., Hollinger, D. Y., Richardson, A. D., Barr, A. G., Beckstein, C., Braswell, B. H., Churkina, G., Desai, A. R., Falge, E., Gove, J. H., Heimann, M., Hui, D., Jarvis, A. J., Kattge, J., Noormets, A., and Stauch, V. J.: Comprehensive comparison of gap-filling techniques for eddy covariance net carbon fluxes, *Agric. For. Meteorol.*, 147, 209–232, <https://doi.org/10.1016/J.AGRFORMAT.2007.08.011>, 2007.

20 Monteith, J. L.: Evaporation and environment, *Symp. Soc. Exp. Biol.*, 19, 205–234, 1965.

Monteith, J. L. and Unsworth, M. H.: Principles of environmental physics, Arnold, London, UK, 1990.

Moss, R. H., Edmonds, J. A., Hibbard, K. A., Manning, M. R., Rose, S. K., van Vuuren, D. P., Carter, T. R., Emori, S., Kainuma, M., Kram, T., Meehl, G. A., Mitchell, J. F. B., Nakicenovic, N., Riahi, K., Smith, S. J., Stouffer, R. J., Thomson, A. M., Weyant, J. P., and Wilbanks, T. J.: The next generation of scenarios for climate change research and assessment, *Nature*, 463, 747–756, <https://doi.org/10.1038/nature08823>, 2010.

25 Novick, K., Oren, R., Stoy, P., Siqueira, M., and Katul, G.: Nocturnal evapotranspiration in eddy-covariance records from three co-located ecosystems in the Southeastern U.S.: Implications for annual fluxes, *Agric. For. Meteorol.*, 149, 1491–1504, <https://doi.org/10.1016/j.agrformat.2009.04.005>, 2009.

Pastorello, G. Z., Agarwal, D. A., Papale, D., Samak, T., Trotta, C., Ribeca, A., Poindexter, C. M., Faybushenko, B., Gunter, D. K., Hollowgrass, R., and Canfora, E.: Observational Data Patterns for Time Series Data Quality Assessment, in: Proc. 10th IEEE Int. Conf. e-Science, pp. 271–278, Sao Paulo, <https://doi.org/10.1109/eScience.2014.45>, 2014.

Penman, H. L.: Natural evaporation from open water, bare soil and grass, *Proc. R. Soc. Lond. A. Math. Phys. Sci.*, 193, 120–145, 1948.

Peters, A., Nehls, T., Schonsky, H., and Wessolek, G.: Separating precipitation and evapotranspiration from noise—a new filter routine for high-resolution lysimeter data, *Hydrol. Earth Syst. Sci.*, 18, 1189–1198, <https://doi.org/10.5194/hess-18-1189-2014>, 2014.

35 Peters, A., Nehls, T., and Wessolek, G.: Technical note: Improving the AWAT filter with interpolation schemes for advanced processing of high resolution data, *Hydrol. Earth Syst. Sci.*, 20, 2309–2315, <https://doi.org/10.5194/hess-20-2309-2016>, 2016.



Peters, A., Groh, J., Schrader, F., Durner, W., Vereecken, H., and Pütz, T.: Towards an unbiased filter routine to determine precipitation and evapotranspiration from high precision lysimeter measurements, *J. Hydrol.*, 549, 731–740, <https://doi.org/10.1016/J.JHYDROL.2017.04.015>, 2017.

Reichstein, M., Falge, E., Baldocchi, D., Papale, D., Aubinet, M., Berbigier, P., Bernhofer, C., Buchmann, N., Gilmanov, T., Granier, A.,
5 Grunwald, T., Havrankova, K., Ilvesniemi, H., Janous, D., Knohl, A., Laurila, T., Lohila, A., Loustau, D., Matteucci, G., Meyers, T.,
Miglietta, F., Ourcival, J.-M., Pumpanen, J., Rambal, S., Rotenberg, E., Sanz, M., Tenhunen, J., Seufert, G., Vaccari, F., Vesala, T., Yakir,
D., and Valentini, R.: On the separation of net ecosystem exchange into assimilation and ecosystem respiration: review and improved
algorithm, *Glob. Chang. Biol.*, 11, 1424–1439, <https://doi.org/10.1111/j.1365-2486.2005.001002.x>, 2005.

Ruth, C. E., Michel, D., Hirschi, M., and Seneviratne, S. I.: Comparative Study of a Long-Established Large Weighing Lysimeter and a
10 State-of-the-Art Mini-lysimeter, *Vadose Zo. J.*, 17, 0, <https://doi.org/10.2136/vzj2017.01.0026>, 2018.

Sellers, P., Randall, D., Collatz, G., Berry, J., Field, C., Dazlich, D., Zhang, C., Collelo, G., Bounoua, L., Sellers, P., Randall, D., Collatz, G.,
Berry, J., Field, C., Dazlich, D., Zhang, C., Collelo, G., and Bounoua, L.: A Revised Land Surface Parameterization (SiB2) for Atmospheric
GCMS. Part I: Model Formulation, *J. Clim.*, 9, 676–705, [https://doi.org/10.1175/1520-0442\(1996\)009<0676:ARLSPF>2.0.CO;2](https://doi.org/10.1175/1520-0442(1996)009<0676:ARLSPF>2.0.CO;2), 1996.

Seneviratne, S. I., Lehner, I., Gurtz, J., Teuling, A. J., Lang, H., Moser, U., Grebner, D., Menzel, L., Schroff, K., Vitvar, T., and Zappa,
15 M.: Swiss prealpine Rietholzbach research catchment and lysimeter: 32 year time series and 2003 drought event, *Water Resour. Res.*, 48,
<https://doi.org/10.1029/2011WR011749>, 2012.

Snyder, K. A., Richards, J. H., and Donovan, L. A.: Night-time conductance in C3 and C4 species: do plants lose water at night?, *J. Exp.
Bot.*, 54, 861–865, <https://doi.org/10.1093/jxb/erg082>, 2003.

Vinukollu, R. K., Wood, E. F., Ferguson, C. R., and Fisher, J. B.: Global estimates of evapotranspiration for climate studies
20 using multi-sensor remote sensing data: Evaluation of three process-based approaches, *Remote Sens. Environ.*, 115, 801–823,
<https://doi.org/10.1016/J.RSE.2010.11.006>, 2011.

Wutzler, T., Lucas-Moffat, A., Migliavacca, M., Knauer, J., Sickel, K., Šigut, L., Menzer, O., and Reichstein, M.: Basic and extensible
post-processing of eddy covariance flux data with REddyProc, *Biogeosciences*, 15, 5015–5030, <https://doi.org/10.5194/bg-15-5015-2018>,
2018.

25 Zeppel, M. J. B., Lewis, J. D., Medlyn, B., Barton, C. V. M., Duursma, R. A., Eamus, D., Adams, M. A., Phillips, N., Ellsworth, D. S.,
Forster, M. A., and Tissue, D. T.: Interactive effects of elevated CO₂ and drought on nocturnal water fluxes in *Eucalyptus saligna*, *Tree
Physiol.*, 31, 932–944, <https://doi.org/10.1093/treephys/tpr024>, 2011.

Zeppel, M. J. B., Lewis, J. D., Chaszar, B., Smith, R. A., Medlyn, B. E., Huxman, T. E., and Tissue, D. T.: Nocturnal stomatal conductance
responses to rising [CO₂], temperature and drought, *New Phytol.*, 193, 929–938, <https://doi.org/10.1111/j.1469-8137.2011.03993.x>, 2012.

30 Zeppel, M. J. B., Lewis, J. D., Phillips, N. G., and Tissue, D. T.: Consequences of nocturnal water loss: a synthesis of regulating factors and
implications for capacitance, embolism and use in models, *Tree Physiol.*, 34, 1047–1055, <https://doi.org/10.1093/treephys/tpu089>, 2014.

Zhang, K., Kimball, J. S., Nemani, R. R., Running, S. W., Hong, Y., Gourley, J. J., and Yu, Z.: Vegetation Greening and Climate Change
Promote Multidecadal Rises of Global Land Evapotranspiration, *Sci. Rep.*, 5, 15 956, <https://doi.org/10.1038/srep15956>, 2015.